Effect of model-form definition on uncertainty quantification in coupled models of mid-frequency range simulations

Kendra L van Buren, Morvan Ouisse, Scott Cogan, Emeline Sadoulet-Reboul, Laurent Maxit

Effect of Model-Form Definition on Uncertainty Quantification in Coupled Models of Mid-frequency Range Simulations

Kendra L. Van Buren[a], Morvan Ouisse[b,*], Scott Cogan[c], Emeline Sadoulet-Reboul[d], Laurent Maxit[e]

[a]*Post-doctoral Associate, Département Mécanique Appliquée, Institut FEMTO-ST, Univ. Bourgogne Franche-Comté, Besançon, France and the Engineering Institute, Los Alamos National Laboratory, Los Alamos, New Mexico, USA*
[b]*Professor, École Nationale Superieure de Mécanique et des Microtechniques-Univ. Bourgogne Franche-Comté, Besançon, France*
[c]*Research Fellow, Département Mécanique Appliquée, Institut FEMTO-ST, CNRS-Univ. Bourgogne Franche-Comté, Besançon, France*
[d]*Associate Professor, Université de Franche-Comté-Univ. Bourgogne Franche-Comté, Besançon, France*
[e]*Associate Professor, Univ Lyon, INSA-Lyon, LVA EA677, F-69621, Villeurbanne, France*

Abstract

In the development of numerical models, uncertainty quantification (UQ) can inform appropriate allocation of computational resources, often resulting in efficient analysis for activities such as model calibration and robust design. UQ can be especially beneficial for numerical models with significant computational expense, such as coupled models, which require several subsystem models to attain the performance of a more complex, inter-connected system. In the coupled model paradigm, UQ can be applied at either the subsystem model level or the coupled model level. When applied at the subsystem level, UQ is applied directly to the physical input parameters, which can be computationally expensive. In contrast, UQ at the coupled level may not be representative of the physical input parameters, but comes at the benefit of being computationally efficient to implement. To be physically meaningful, analysis at the coupled level requires information about how uncertainty is propagated through from the subsystem level. Herein, the proposed strategy is based on simulations performed at the subsystem level to inform a covariance matrix for UQ performed at the coupled level. The approach is applied to a four-subsystem model of mid-frequency vibrations simulated using the Statistical Modal Energy Distribution Analysis, a variant of the Statistical Energy Analysis. The proposed approach is computationally efficient to implement, while simultaneously capturing information from the subsystem level to ensure the analysis is physically meaningful.

Keywords: uncertainty quantification, statistical energy analysis, statistical modal energy distribution analysis, model reduction

1. Introduction

In design and analysis, numerical models have traditionally been pursued to gain insight into the performance of structures that are costly to build, potentially shortening the design-build-test cycle. With modern-day computing resources, it is now possible to develop more complex numerical models that are capable of incorporating a higher fidelity representation of physics processes at resolutions that were previously impossible to achieve. In particular, it has become common to pursue coupled models, whereby several numerical models are utilized to represent the overall behavior of a more complex, inter-connected system. Herein, coupled models are those models whose physics processes are simulated utilizing two or more numerical models, of either the same or differing physics. The output of the individual numerical models are then integrated to obtain the desired quantities of interest. Such examples can include sub-structuring analysis of a finite element (FE) simulation, or pursuing fluid-structure interaction with computational fluid dynamics and FE simulations. It is emphasized, however, that there are unavoidable sources of assumptions and uncertainty in the development of these numerical models that must be accounted for so that they can be used reliably for decision-making purposes. In the development of these numerical models, assumptions enable model development but simultaneously limit the ability of the model to replicate reality.

*morvan.ouisse@femto-st.fr

The desire to utilize numerical models in a predictive capacity has given rise to uncertainty quantification (UQ), which is a field of research that focuses on understanding how predictions of a numerical model are affected by sources of uncertainty and assumptions inherent to the model. Such activities that contribute toward uncertainty quantification include parametric studies, effect screening, sensitivity analysis, and the forward propagation of uncertainty, the goals of which contribute to efficient numerical optimization and robust design. Thus far, UQ has gained much maturity for models that require only one forward calculation. UQ of coupled numerical models has received some attention in the published literature, however, it will undoubtedly continue to receive scientific interest due to the increased sources of assumptions that are necessary in order to couple several models together.

The basic flowchart of the coupled model paradigm addressed in this manuscript is outlined in Figure 1. This coupled model paradigm is commonly referred to as a *weakly coupled* model, where subsystem models are used to generate inputs for coupled models. This is unlike *strongly coupled* models where there can be feedback between models at the subsystem and coupled model levels. There are two levels of analysis that are identified in the figure. The first level of analysis is where N subsystem models, $y_{s,i} = f_{s,i}(\theta_{s,i}; p_{s,i})$, $i = 1...N$, are defined. Uncertain calibration parameters, $\theta_{s,i}$, are those that are introduced by environmental conditions and modeling choices whereas control parameters, $p_{s,i}$, are dimensions of the parameter space controlled by the analyst. The subsystem models serve an integral purpose in order to calculate the final quantities of interest, for example, use of a computational fluid dynamics code that might be used to determine forces that are applied to a finite element model, or a micro-scale model of material behavior used to characterize the stress-strain characteristics of a macro-scale material model. The subsystem level is thus the first level way of considering a system to compute primary responses of the system that will serve the second level named the coupled level.

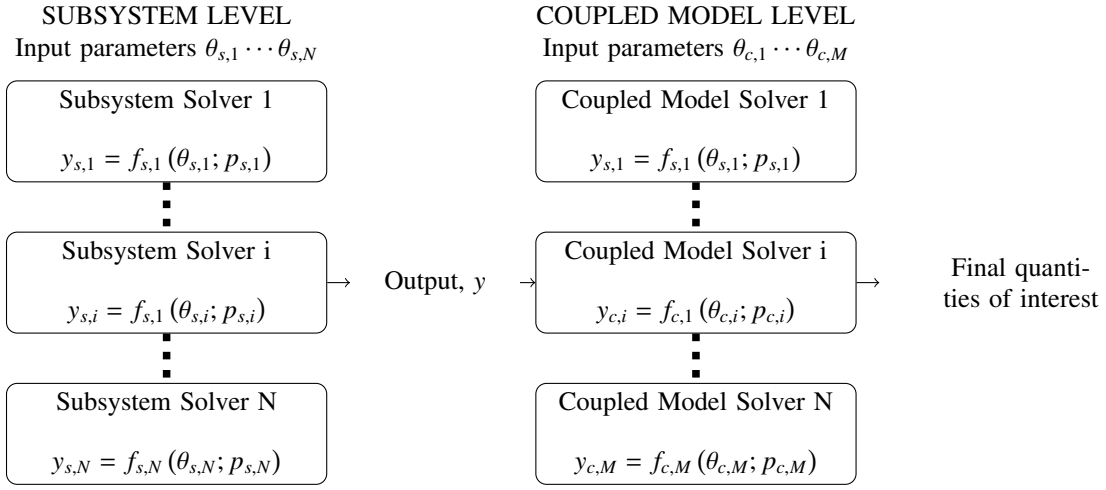

Figure 1: Levels of Uncertainty of Coupled Models.

Generated from the subsystem models are outputs, y, which are then used to define the inputs for the M coupled model solvers, as indicated in Figure 1. Note that there can be a different number of coupled models, $y_{c,i}$ than there are of subsystem models, $y_{s,i}$. The coupled model solvers are then used to obtain the final quantities of interest. In addition, there may be multiple levels of coupled models before arriving at the final quantities of interest, for example, one that might go from micro- to meso- to macro-scale behavior of a material.

Extending UQ activities to coupled models is not as straightforward as it is with numerical models that require only one forward calculation. Coupled simulations can be computationally more expensive to execute, and can be defined using different model forms or structures. For example, in the coupled model framework illustrated in Figure 1, one can envision that uncertainty can be introduced using either the parameters at the subsystem level, $\theta_{s,i}$, or parameters at the coupled model level, $\theta_{c,i}$. In this sense, the numerical model can be defined using the subsystem level model form or the coupled level model form. At the subsystem level the parameters may have a physical meaning, such as material density or geometry, suggesting that UQ at this level will carry a physically meaningful interpretation. However, this approach may be cost prohibitive to perform due to the computational expense required to execute the

subsystem models several times. In comparison, UQ at the coupled model level is computationally cheaper to perform but at the risk that the results will lose physical meaning.

One analysis that may be considered as a coupled model simulation is the Statistical Energy Analysis (SEA), and some of the alternative methodologies that have been inspired by SEA for studying the mid- to high- frequency vibration response of structures. SEA was first developed for application to satellite launch vehicles and has since been extended to other applications, for example the design of cars, trains, and satellites [1, 2, 3]. The goal of SEA is not to provide a high-fidelity simulation but rather to provide a statistical average of the vibratory behavior of the structure of interest [4]. The basic premise of SEA is to reduce a structure down to single degree of freedom (SDOF) oscillators that are analyzed through their subsystem responses. SEA offers computational efficiency by analyzing SDOF oscillators, however, this simplification comes at the cost of losing spatial resolution of the system response. The main assumptions needed for the analysis have been widely acknowledged [5] and include: (i) the need for a large population of modes in the frequency band of interest (contested in [6]), (ii) modal equipartition, meaning that no mode dominates the energy in the frequency band, (iii) the ratio of the coupling loss factor to the internal loss factor is low, (iv) coupling between subsystems must be conservative, and (v) excitation must be wide-band, spatially distributed and uncorrelated. Despite these assumptions, the method has been shown to work well in several applications, however, different aspects of the method have been questioned due to the numerous assumptions.

To remedy the assumption of modal equipartition an alternate approach known as the Statistical Modal Energy Distribution Analysis (SmEdA - the S, E, and A remain capitalized to emphasize its roots in the SEA approach) has been proposed [7, 8]. SmEdA is one of several strategies developed to extend the statistical approaches to lower frequencies and tackle the mid-frequency problem such as the Asymptotic Scaled Modal Analyses based on scaling procedures [9, 10], or the Energy Distribution Methods [11] that propose alternatives to compute the SEA parameters. SmEdA utilizes natural frequencies and mode shapes of the subsystems used to drive the analysis, rather than approximating the behavior of a structure using SDOF oscillators as is done in SEA. The natural frequencies and mode shapes are typically obtained through FE analysis, however, any form of analysis, experimental or analytic, can be utilized to provide modal information. When the SmEdA framework is implemented analytically, it can be considered as a coupled model as described in Figure 1 whereby the material and geometric definition of the numerical model define the subsystem level, and the natural frequencies and mode shapes define the coupled model level. Unlike in SEA, the spatial information of the structure is retained and has the potential to contribute toward design criteria. Although SmEdA overcomes the assumption of modal equipartition there are still several assumptions that are utilized in the analysis that should be accounted for.

The goal of this manuscript is to compare the sensitivity analysis and uncertainty propagation of a structure simulated in the SmEdA framework at both the subsystem and coupled levels. It is proposed to use a covariance matrix that is informed by simulations at the subsystem level to perform uncertainty propagation at the coupled level. The basic question to answer is: *can analysis at the coupled model level provide physically meaningful results?* How to develop an uncertainty model at the coupled model level that properly reflects the uncertainty introduced at the subsystem level, and the extent to which simulations defined at the subsystem level to inform a non-parametric uncertainty model are needed is also addressed. The analysis is demonstrated on a four subsystem numerical model, originally developed to demonstrate SmEdA [7] and slightly modified herein. The numerical mid-frequency model is hence validated and used in this paper to illustrate the methodologies. The remainder of the manuscript is organized as follows. A brief review of uncertainty quantification efforts, especially those pertaining to SmEdA, are discussed in Section 2. Section 3 provides in-depth background of the techniques utilized herein, including SEA, SmEdA, effect screening, and uncertainty propagation. The four subsystem numerical model is described in Section 4, along with a comparison of UQ results obtained herein. Overall conclusions and suggestions for future work are presented in Section 6.

2. Literature Review

The use of uncertainty quantification (UQ) techniques has long been pursued to understand the effects that sources of uncertainty have on model-based decisions. In modeling and simulation applications, UQ typically entails the use of parametric studies, whereby ”sources of uncertainty” refer to those defined by the model parameters. These techniques manifest themselves in effect screening, sensitivity analysis, and stochastic model updating, and have

become an essential part of the model development process [12, 13, 14]. As such, textbooks devoted to the topic, for example References [15], [16], have been developed.

Most applications that consider UQ involve model formulations whereby the model requires one forward calculation to obtain the output of interest. There are a vast number of successful studies implementing UQ in the literature, especially for structural dynamics applications pursued with finite element models [17, 18]. There are also instances where UQ has been extended to coupled model simulations, however, in many cases assumptions are utilized to justify introducing uncertainty at either the subsystem model level or at the coupled model level, for example in [19]. The main issue with UQ studies is that they can be computationally expensive to conduct due to the need to sample the model several times with different settings of the input parameters. When trying to identify parameters most influential to model output, two types of analyses can be performed: effect screening, whereby the parameters are ranked qualitatively, and sensitivity analysis, whereby parameters are ranked quantitatively. The motivation for pursuing an effect screening technique originates in the reduced computational demand. In the analysis of coupled numerical models, the computational expense is often an important factor to consider thus making effect screening techniques more attractive, however, it is important to utilize best practices to ensure the results are defensible [20].

The importance of pursuing UQ studies has been acknowledged in the simulation of numerical models within the medium-frequency range as the effects of uncertainties increase with frequency. Some previous studies based on parametric or non-parametric processes have been dedicated to the UQ in the statistical energy analysis (SEA) framework, however, UQ has yet to be extended to the statistical modal energy distribution analysis (SmEdA) framework. In SEA, it is necessary to reduce a structure into single degree of freedom subsystems and then couple them together utilizing coupling loss factors (CLFs) and internal loss factors (ILFs). The CLF and ILF values can vary based on the definition of the subsystems, and changing the CLF and ILF values can impact the SEA energy predicted by the analysis. In Reference [21], the authors propose an approach to find a robust estimation of the CLFs taking into account the variation in the subsystem properties. The authors utilize a combination of finite element (FE) modeling and component mode synthesis to approximate the CLF values. An important assumption, however, is that the authors claim that the choice of exercising variability on the physical properties of the FE model, component modal properties, or system modal properties may be unimportant, and that it is important to include some randomness rather than assume a mean performance of the CLF based on FE analysis. Using this assumption, the authors are able to perform only one FE analysis and draw random modal statistics to propagate in their model. In [22] the stochastic finite element method which consists in representing in a parametric and probabilistic form random uncertainties [23] has been extended to upper frequency applications using the energy operator approach for model reduction.

Another approach to considering the effect of random variability is in Reference [24], where the authors analytically incorporate statistics into the SEA equations as a convenient alternative to parametric studies to predict the response statistics of the method. The authors demonstrate that doing so makes it possible to evaluate the robustness of existing vehicle design to variations in the design parameters, and propose utilizing the information acquired for the development of future designs. In [25] a nonparametric probabilistic model is used for the reduced matrices involved in the dynamic equations and combined with the matrix model developed for the medium-frequency range. References [26] and [27] both consider how the predicted energies will vary as the model inputs are allowed to vary. In Reference [26], the CLF's and ILF's are propagated through the model using a central composite design of experiments. Sensitivity coefficients are then obtained by fitting a regression model according to the output from the Central Composite Design to determine the parameters most influential to the calculated SEA energies. In Reference [28, 27], the authors pursue methods to predict the lower and upper bounds of predictions given that the input parameters are allowed to vary and treated in a non-deterministic way. The parameters include the material properties (Young's modulus, density), physical properties (speed of sound), and the internal loss factors of SEA. Two approaches are pursued: (i) a two-level, full-factorial sampling method, and (ii) by sampling data to train a polynomial metamodel, which is subsequently utilized to find the minimum and maximum performance values of the simulation. The approaches are successfully demonstrated using three applications: (i) a system of two linear equations, (ii) a two subsystem problem used to predict performance of a plate-acoustic system, and (iii) a three subsystem problem used to predict sound transmission loss of a plate. However, the methods proposed by [27] have the potential to be computationally expensive once applied to more computationally demanding numerical models.

In References [21] and [26], heavy emphasis is placed on reducing computational demand of the simulation by using simplifying assumptions to justify the level at which UQ studies are performed. Herein, the goal is to study more directly whether the assumptions are warranted by comparing analysis performed at the subsystem level with

analysis performed at the coupled model level.

3. Methodology

The basic question addressed in this paper is the level at which parametric studies should be applied for UQ of coupled models. Herein, the analysis is applied to the simulation performed in the framework of SmEdA, however, the approach is flexible enough that it can be applied to other coupled model frameworks that follow the formulation outlined in Figure 1. The approaches pursued previously in [26] and [21] have already demonstrated that it is possible to propagate uncertainty in a computationally efficient way within the statistical energy analysis (SEA) framework, by considering the coupling loss factors (CLFs) used at the coupled level of the formulation. This study verifies whether the resulting uncertainty on the outputs of interest are in fact representative of the uncertainty that would be obtained if the subsystem parameters had been utilized.

The flowchart of activities performed in this manuscript are highlighted in Figure 2. The mathematical background needed for each step of the flowchart is discussed in this section such that the manuscript is self-contained; references are provided if the reader wants more in-depth explanations. The first step is to develop the numerical model. As mentioned, the numerical model will utilize the mathematical formulation of SmEdA, which is introduced in Section 3.1. The next step of the analysis is to perform a mesh refinement study to ensure that the mesh discretization is converged, as discussed further in Section 3.2. The resulting numerical model defined at the subsystem level of the coupled model formulation is then sampled in order to provide the information necessary to pursue effect screening. The mathematical formulation for three effect screening techniques pursued herein is provided in Section 3.3: (i) finite differences, (ii) correlation coefficients, and (iii) Morris method. The sampling utilized for effect screening also provides the information necessary to generate a covariance matrix to inform the sampling performed at the coupled model level. The rationale for utilizing a covariance matrix to inform the uncertainty propagation at the coupled model level is discussed further in Section 3.4.

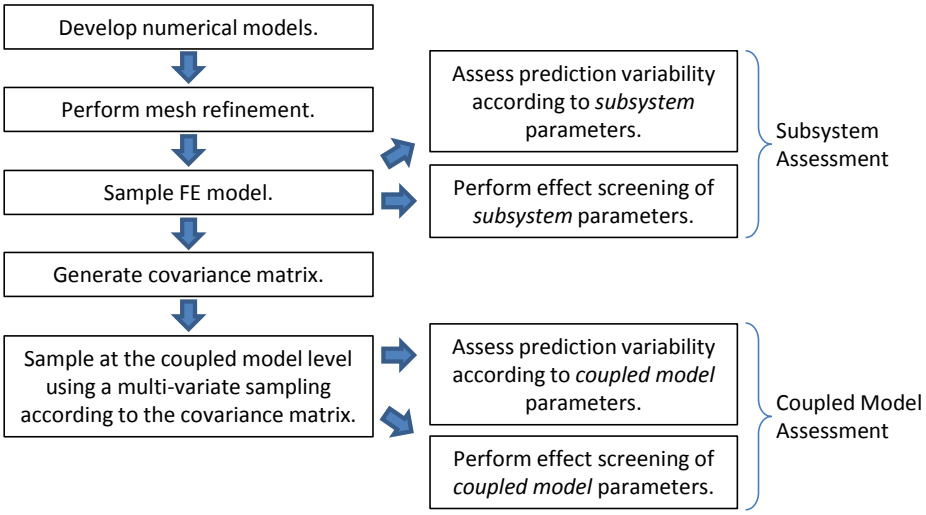

Figure 2: Proposed Flowchart to Assess Model Uncertainties.

3.1. SmEdA

The mathematical formulation of SmEdA is rooted in SEA, whereby it is assumed that the high-frequency response of a set of N subsystems can be described using a linear set of equations:

$$\{\Pi_{inj}\}_{N\times 1} = \{\Pi_{i,d}\}_{N\times 1} + \{\Pi_{ij}\}_{N\times 1}, \tag{1}$$

where Π_{inj} represents the power injected into the system, $\Pi_{i,d}$ represents the power dissipated in subsystem i, and Π_{ij} represents the power transmitted from subsystem i to subsystem j. Approximating the energy balance of the

subsystems as represented in Equation (1) requires the use of internal loss factors to define the power dissipation, and coupling loss factors to define the power transmission. Doing so results in the representation:

$$\Pi^{i}_{inj} = \omega_c \eta_i E_i + \omega_c \sum_{j=1, j\neq i}^{N} (\eta_{ij} E_i - \eta_{ji} E_j), \tag{2}$$

where ω_c is a scalar value representing the center of the frequency band of interest, η_i is the internal loss factor (ILF) of subsystem i, η_{ij} is the coupling loss factor (CLF) between subsystems i and j, and E_i and E_j are the energies of subsystem i and j, respectively.

Consider the case with two subsystems only within the frequency band centered around ω_c, where M_1 is the number of modes in the first subsystem and M_2 is the number of modes in the second subsystem. SEA assumes that each mode will contribute equally to the overall response of the structure, thus the contribution of the modal energy is determined through the ratio of the number of modes, as shown in Equations (3) and (4):

$$\Pi^{1}_{inj} = \omega_c \eta_1 E_1 + \omega_c \eta_{12} \left(E_1 - \frac{M_1}{M_2} E_2 \right), \tag{3}$$

$$\Pi^{2}_{inj} = \omega_c \eta_2 E_2 + \omega_c \eta_{12} \left(\frac{M_1}{M_2} E_2 - E_1 \right). \tag{4}$$

In contrast, SmEdA removes the assumption of modal equipartition, such that the contribution of each mode to the overall response is accounted for individually. SmEdA takes advantage of the dual modal formulation to consider the physical local modes of the same subsystem. Thus, the formulation considers individual modal energies of each subsystem, rather than overall subsystem energies. The resulting formulation is shown in Equations (5) and (6):

$$\Pi^{p}_{inj} = \left(\omega_p \eta_p + \sum_{q=1}^{M_2} \omega_c \eta_{pq} \right) E_p - \sum_{q=1}^{M_2} \omega_c \eta_{pq} E_q, \ \forall p \in [1, ..., M_1], \tag{5}$$

$$\Pi^{q}_{inj} = - \sum_{p=1}^{M_1} \omega_c \eta_{pq} E_p + \left(\omega_q \eta_q + \sum_{p=1}^{M_1} \omega_c \eta_{pq} \right) E_q, \ \forall q \in [1, ..., M_2]. \tag{6}$$

where p and q are modes of subsystems 1 and 2, respectively, with corresponding natural frequencies, ω_p and ω_q. Note that in the SmEdA formulation, the internal loss factors, η_p and η_q, and the coupling loss factors, η_{pq}, are formed for each *modal pair* rather than for each subsystem pair. In addition, the coupling is gyroscopic because there are no mass and stiffness terms that store energy. As a result, the subsystem energies are determined as sums of the modal energies, as shown in Equation (7):

$$E_1 = \sum_{p=1}^{M_1} E_p, \quad E_2 = \sum_{q=1}^{M_2} E_q. \tag{7}$$

The formulation presented in Equations (5-7) can be extended to the prediction of more than two subsystems. As discussed further in References [7] and [8], satisfying the SmEdA formulation requires that there is a rupture of impedance between subsequent subsystems models, where the simulation is obtained from the uncoupled simulation of the subsystems using free or blocked boundary conditions.

The three levels of the SmEdA analysis are illustrated in Figure 3. The first level is the subsystem level defined using finite element models where the material and geometric properties are defined. The next level is to consider the natural frequencies, ω, and mode shapes, ϕ, as determined from the FE analysis at the subsystem level, and the last level is defined using the CLF's and ILF's to obtain the subsystem energies. It should be emphasized that, in this work, no uncertainty is introduced on damping as it is generally introduced in the same way at the subsystem and at the coupled model levels so that uncertainties on this parameter does not lead to a difference between the two levels considered. Moreover, a specific distribution law, such as a log-normal distribution, could be more relevant for damping than a uniform distribution. Depending on the physics, in some cases uncertainties in the DLFs might

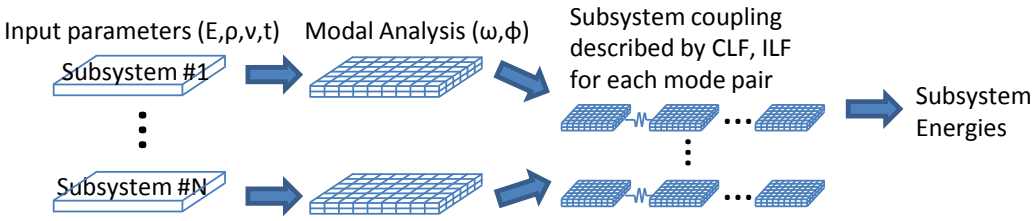

Figure 3: Levels in the SmEdA Analysis at which Uncertainty Quantification can be Performed.

dominate the energy dispersion response. In this case, the influence of the other physical parameters would not be visible at the coupled model levels, which is the main objective of the paper.

It is more desirable to perform UQ using the subsystem parameters because it is possible to physically interpret the results. For example, if a parametric study of the thicknesses of the different subsystems is pursued, UQ techniques would be able to determine which subsystem thickness has the greatest effect in either reducing or increasing the produced vibratory energy. Knowing which subsystem is most influential to the produced energy would be potentially useful information for the designer, however, parametric study at the subsystem level can be computationally expensive because of the need to execute the FE model for every calculation.

In comparison, UQ at the coupled model levels is still able to provide meaningful information about more global properties of a model. Analysis at the coupled level comes with the benefit of being computationally trivial to solve in comparison to analysis at the subsystem level because it is no longer necessary to execute the FE model; rather, only the SmEdA equations need to be solved. In the SmEdA framework there are two coupled model levels that can be utilized: (i) the modal coupling loss factors (CLF) and internal loss factors (ILF), or (ii) the mode shapes and frequencies used to calculate the CLFs and ILFs. Perturbing only the CLF or ILF would be straightforward and computationally efficient to pursue, as demonstrated previously [26, 21] within the SEA framework. The question that remains is how to physically interpret what it means to increase or decrease CLF and ILF values, and if the range of variation assumed in a UQ study is representative of perturbation in the physical input parameters. The other option is to perturb the mode shapes and frequencies. Doing so has the potential to provide a physical interpretation because they can be related to the mass and stiffness of a structure. The same issue of whether the amount of variation assumed in the coupled model parameters is representative of variation in the subsystem input parameters still arises. Herein, a covariance matrix is implemented to help mitigate this difficulty due to the fact that it can help to inform sampling performed at the coupled model level using the results of sampling performed at the subsystem level.

3.2. Mesh Refinement

Herein, finite element analysis is utilized to provide the natural frequencies and mode shapes to the SmEdA analysis. Any time that a numerical method, such as the finite element method, is implemented it is important to determine if an appropriate mesh discretization is being defined to represent the continuous differential equations. The purpose of a mesh refinement study is to assess that the level of mesh discretization utilized is significantly resolved such that the truncation error has an acceptably small effect on the solution. Criteria for adequate refinement based notably on the wavelength exist when considering simple homogeneous geometries but these criteria are not always relevant when considering complex geometries and do not exist at at all for coupled levels. In-depth derivation and discussion of the steps needed for a mesh refinement study can be found in [29]. The truncation error of the simulation is defined using the Ansatz error model :

$$\varepsilon(\Delta x) = |y^{Exact} - y| = \beta \Delta x^p + O(\Delta x^{p+1}) \tag{8}$$

where $\varepsilon(\Delta x)$ denotes the user-defined error metric between the exact solution y^{Exact} and the discrete solution y obtained using a grid size Δx. The pre-factor β is a constant regression coefficient, the exponent p is the rate of convergence of the truncation error as the mesh size is resolved, and $O(\Delta x^{p+1})$ represents the higher order terms.

The exact solution of the code is often only available when performing simple calculations; for more complex simulations it becomes necessary to approximate the exact solution of Equation (8) with a reference solution, denoted herein as y^{ref}. This approximation can be achieved utilizing the well-known Richardson extrapolation, which requires

the simulation results of the code at three levels of mesh resolution: (Δx_C), used to denote the coarse-grid resolution; (Δx_M), used to denote the medium-grid resolution; and (Δx_F), used to denote the fine-grid resolution. For simplicity, it is the most straightforward to perform mesh refinement when there is a constant refinement ratio between the coarse, medium, and fine grid resolutions, as shown in Equation (9):

$$R = \frac{\Delta x_C}{\Delta x_M} = \frac{\Delta x_M}{\Delta x_F}. \tag{9}$$

The ratio of solution differences, denoted herein as ξ is also required, and can be used to define the rate of convergence of the solution, denoted herein as p, as shown in Equation (10):

$$\xi = \frac{y(\Delta x_M) - y(\Delta x_C)}{y(\Delta x_F) - y(\Delta x_M)}; \quad p = \frac{\log(\xi)}{\log(R)}. \tag{10}$$

Finally, the Richardson extrapolation can be approximated as shown in Equation (11), which can be used to calculate the truncation error of Equation (8):

$$y^{ref} = y(\Delta x_F) + \frac{y(\Delta x_F) - y(\Delta x_M)}{R^p - 1} = y(\Delta x_M) + \frac{y(\Delta x_M) - y(\Delta x_C)}{R^p - 1}. \tag{11}$$

Lastly, it is noted that a mesh refinement study simply verifies the convergence of the system of partial differential equations used to define a numerical model. There are two main caveats: (i) the study only assesses the ability to *self-converge*, and there is no way to verify that the extrapolated solution, y^{ref} is consistent with the exact solution, y^{Exact}, and (ii) there is no guarantee that the equations will hold when applied to the simulation of coupled numerical models.

3.3. Effect Screening Techniques

As mentioned, the SmEdA model is dependent on several variables, which each contribute to the output of interest. Herein, the question is to determine which variables are most influential to the model output using three different effect screening techniques: (i) finite differences approach, (ii) correlation coefficients, and (iii) the Morris method. The mathematical formulation of the techniques pursued are presented in this section for completeness; more detailed explanations and theoretical discussion can be found in [16].

3.3.1. Finite Differences Approach

The finite differences approach provides a local measure of sensitivity. As such, it is widely discouraged to pursue when other, more accurate global effect screening techniques are computationally feasible [12]. Herein, a finite differences approach is simply pursued as a comparison; the goal is to demonstrate whether a local sensitivity analysis is capable of providing an accurate approximation of a global analysis.

The finite difference procedure ranks the influence of parameters θ as each parameter, θ_j, is perturbed one at a time by $\Delta\theta_j$, as suggested in Equation (12):

$$\frac{\partial y}{\partial \theta_j} \approx \frac{y(\theta_j + \Delta\theta_j) - y(\theta_j)}{\Delta\theta_j}. \tag{12}$$

The basic idea is that the larger the change in output, y that is produced from the change in parameter θ_j, the more influential θ_j is to the output. Parameter ranking using this methodology requires $j + 1$ simulations, where j is the number of parameters used to define the simulation.

3.3.2. Correlation Coefficients

Correlation coefficients provides a measure of sensitivity utilizing sampling obtained from a computational design of experiments. Suppose that there are m simulation predictions that can be utilized. The correlation coefficient, $r_{\theta y}$, which is utilized to calculate the influence of parameter θ on the output y, is calculated as shown in Equation (13):

$$r_{\theta y} = \frac{\sum_{k=1}^{m} (\theta - \bar{\theta})(y_k - \bar{y}))}{\left[\sum_{k=1}^{m} (\theta_k - \bar{\theta})^2\right]^{1/2} \left[\sum_{k=1}^{m} (y_k - \bar{y})^2\right]^{1/2}}, \tag{13}$$

where

$$\bar{\theta} = \sum_{k=1}^{m} \frac{\theta_k}{m}; \qquad \text{and} \qquad \bar{y} = \sum_{k=1}^{m} \frac{y_k}{m}. \tag{14}$$

When the correlation coefficient is positive, the input parameter is positively correlated with the output, and negative suggests a negative correlation. Further, the larger the correlation coefficient, the more influential the parameter, θ is to the output, y.

3.3.3. Morris Method

The Morris method is a technique for effect screening that was first introduced by [30] and later improved by [31]. Although only providing a qualitative measure of sensitivity, it has been shown to work well with problems defined in large-dimensional spaces due to its computational efficiency.

The Morris method relies on evaluating the elementary effects of "trajectories" constructed within the input space. The elementary effect is defined as the influence of moving one parameter at a time within the parameter space used to define the simulation, as shown in Equation (15):

$$EE_{\mathrm{k}}^{(r)} = \left| \frac{y(\theta_1^{(r)}, ..., \theta_{\mathrm{k}}^{(r)} + \Delta\theta_{\mathrm{k}}^{(r)}, ..., \theta_{\mathrm{D}}^{(r)}) - y(\theta_1^{(r)}, ..., \theta_{\mathrm{k}}^{(r)}, ..., \theta_{\mathrm{D}}^{(r)})}{\Delta\theta_{\mathrm{k}}^{(r)}} \right|, \tag{15}$$

where $EE_k^{(r)}$ is the elementary effect of the k^{th} parameter in the r^{th} trajectory, $\Delta\theta$ is the amount that the parameter θ is perturbed, and D is the number of parameters used to define the simulation.

The construction of trajectories within the parameter space is similar to other "one-at-a-time" methods, such as the finite difference approach discussed previously with the exception that the amount each parameter is perturbed is no longer infinitesimal. The Morris method provides a reliable approximation of the global statistics due to the fact that multiple trajectories with random origins in the input space are constructed [20]. Each trajectory requires (D+1) simulations, where D is the number of parameters used to define the simulation. Reference [31] suggests the use of 10-50 trajectories in order to provide converged statistics for ranking the parameters. The number of simulations required to construct a trajectory suggests that the number of necessary simulations will increase linearly as the number of parameters increases. It is for this reason that the Morris method has the potential to significantly reduce computational expense, because other global sensitivity analysis techniques such as an analysis of variance might require the number of simulations increase exponentially as the number of parameters increases. The construction of two trajectories defined in a two-dimensional parameter space is shown in Figure 4.

The mean and standard deviation statistics of the elementary effects, provided in Equations (16) and (17), respectively are used to rank the influence of the parameters. Large values of the mean suggest that the parameter is highly influential to the model output, whereas large values of the standard deviation suggest that the parameter is non-linear with interactions to other parameters:

$$\mu_k(EE) = \frac{1}{N} \times \sum_{1 \le r \le N} EE_{\mathrm{k}}^{(r)} \tag{16}$$

$$\sigma_k(EE) = \sqrt{\frac{1}{N-1} \times \sum_{1 \le r \le N} (EE_{\mathrm{k}}^{(r)} - \mu_k(EE))^2}. \tag{17}$$

3.4. Propagation of Uncertainty

Sampling of the uncertain input parameters is pursued to assess the overall influence of the input parameters to the quantities of interest. It is noted, that the sampling techniques pursued in the current study are limited to those that are computationally feasible to implement. Herein, Monte Carlo (MC) sampling is utilized to sample the uncertain input parameters used to define the SmEdA analysis. Note that the sampling can be performed directly to the parameters, or to the hyper-parameters of a probability law used to describe a parameter. MC sampling is fairly straightforward to implement: the domain of possible values for input parameter values are defined and values are randomly sampled to characterize the output uncertainty. When sampling in a space defined by multiple calibration parameters, it may

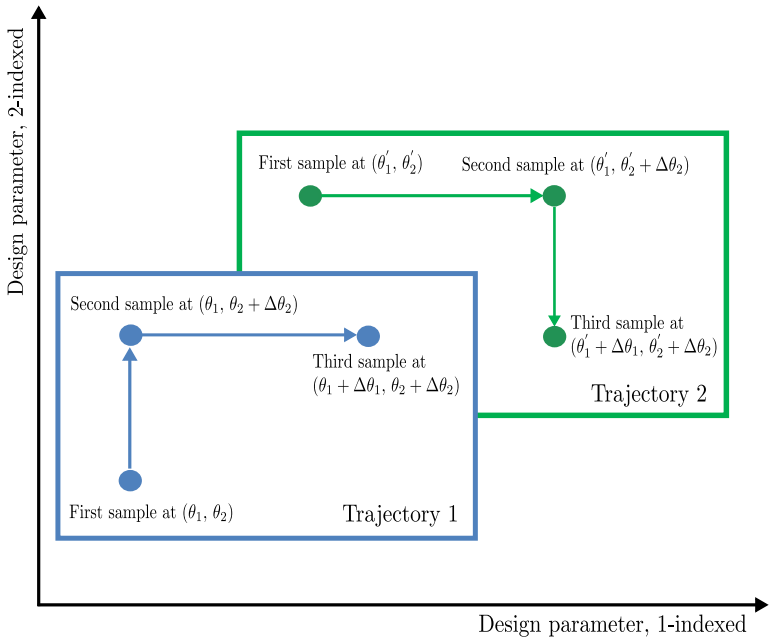

Figure 4: Construction of Morris Trajectories in Two-Dimensional Space.

be useful to assume a multi-variate normal distribution and sample according to the mean and covariance matrix used to define the distribution. In this case, sampling the uncertain probability distribution would be done according to the expression provided in Equation (18):

$$x = \mu + Az, \tag{18}$$

where x is the random vector used to sample the model, μ is the vector of mean values of the parameters, A is a real matrix obtained from the covariance matrix, and z is a vector of standard normal variates obtained using a multi-variate random number generator. The matrix, A, is obtained from the covariance matrix, Σ, in a way that satisfies the relationship shown in Equation (19):

$$\Sigma = AA^T. \tag{19}$$

The matrix, A can typically be obtained using a Cholesky decomposition, or a spectral decomposition, depending on if the covariance matrix is positive semi-definite. It is also noted that the sampling suggested in Equations (18-19) will hold true to provide a uni-variate normal distribution, where μ would be a scalar value and A would be the scalar standard deviation.

4. Case-study Application

Having provided the mathematical description for techniques utilized in this manuscript in Section 3, application to a four-subsystem numerical model is now pursued. The goal is to draw comparison between the analysis performed at the subsystem level and at the coupled model level. The four-subsystem model pursued herein is adapted from the numerical model developed in [7] and is shown in Figure 5. The model consists of four subsystems: (i) a 1 m by 1.5 m by 3 mm plate, (ii) a 1 m by 0.7 m by 2 mm plate situated at a 90° angle from the first plate, (iii) a 1 m by 1.1 m by 6 mm plate situated at a 90° angle from the second plate, and (iv) a 1 m by 2.3 m by 3 mm plate situated at a 90° angle from the third plate. Herein, excitation is applied to subsystems #1 and #3 in the frequency band 1410-1780 Hz, which is in the MF range for the structure of interest and which is the frequency band utilized for all results provided.

The model is developed in Patran 2012 FE preprocessing software using PSHELL elements and linear, isotropic material properties, and FE analysis is performed using Nastran. The model parameters are listed in Table 1, where each subsystem is defined by a Young's modulus, density, Poisson's ratio, and thickness. A constant damping ratio

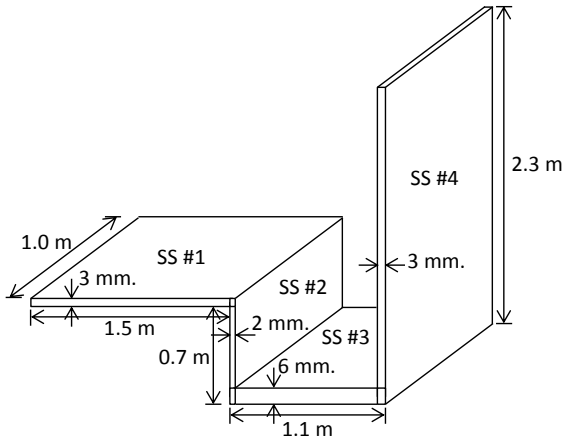

Figure 5: Four-subsystem model.

of 0.05 is assumed for all subsystems. The evolution of the plate modal overlap factors with frequency is presented in figure 6. The study is carried out in the frequency band between 1410 and 1780 Hz where modal overlap factors are around and more than 1 justifying a hybrid approach such as SmEdA. To solve for the vibratory energies in the SmEdA framework from the subsystem level, the FE model of each subsystem model is executed, and the relevant mode shapes and natural frequencies are extracted to provide the information necessary to calculate the modal CLF's and ILF's. In turn, the CLF's and ILF's can be used to solve for the vibratory energies within the SmEdA framework as defined in Equations (5 - 7). Evaluating the energy of each model from the subsystem level takes approximately 3 minutes utilizing parallel computing such that all four FE calculations are performed simultaneously on a cluster computing network with 8 GB of RAM for each FE calculation.

Table 1: Physical Parameters Defined at the Subsystem Level.

Number	Parameter	Abbreviation	Nominal Value
1	SS# 1: Young's Modulus $[m^{-1} \cdot kg \cdot s^{-2}]$	E_1	2e11
2	SS# 1: Density $[kg \cdot m^{-1}]$	ρ_1	7800
3	SS# 1: Poisson's Ratio	ν_1	0.3
4	SS# 1: Thickness [m]	t_1	0.003
5	SS# 2: Young's Modulus $[m^{-1} \cdot kg \cdot s^{-2}]$	E_2	2e11
6	SS# 2: Density $[kg \cdot m^{-1}]$	ρ_2	7800
7	SS# 2: Poisson's Ratio	ν_2	0.3
8	SS# 2: Thickness [m]	t_2	0.002
9	SS# 3: Young's Modulus $[m^{-1} \cdot kg \cdot s^{-2}]$	E_3	2e11
10	SS# 3: Density $[kg \cdot m^{-1}]$	ρ_3	7800
11	SS# 3: Poisson's Ratio	ν_3	0.3
12	SS# 3: Thickness [m]	t_3	0.006
13	SS# 4: Young's Modulus $[m^{-1} \cdot kg \cdot s^{-2}]$	E_4	2e11
14	SS# 4: Density $[kg \cdot m^{-1}]$	ρ_4	7800
15	SS# 4: Poisson's Ratio	ν_4	0.3
16	SS# 4: Thickness [m]	t_4	0.003

In comparison, evaluation of the vibratory energies from the coupled model level foregoes use of the FE model and requires only the natural frequencies and mode shapes of each subsystem to be defined. Recall, from Equation (7), that the SmEdA energies are summed over the modal pairs of subsystems within the frequency band. It can be expected that mode swapping can occur during the parametric study, however, the form of the spatial mode shapes

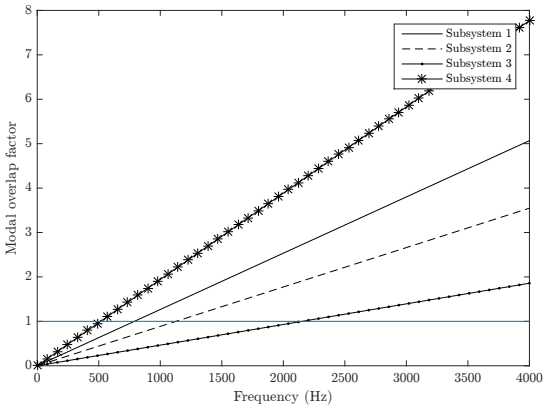

Figure 6: Evolution of the modal overlap factor with frequency for each plate subsystem.

stays consistent such that the modes can be tracked. When the model parameters are allowed to vary, the mode shapes appearing within the frequency band may drift out, and likewise, mode shapes originally outside of the frequency band may drift in. To track these mode shapes, the frequency band is expanded to save the bases of modal frequencies that drift in and out of the frequency band of interest, as discussed further in Section 4.3. Clearly, parametric study of all the potential modal frequencies may easily outnumber the sixteen parameters that are identified at the subsystem level. Further, randomly sampling the modal frequencies and associated spatial mode shapes would lose information about the relative spacing between mode shapes. For these reasons, it is proposed to utilize a covariance matrix to inform the multivariate sampling of the natural frequencies. The computational benefit of applying the parametric study to the natural frequencies despite the increase in number of parameters must be emphasized: evaluation of the vibratory energies from the coupled level takes approximately 0.04 seconds to perform in MATLAB on a standard dual-core laptop with 8 GB of RAM, about 720 times speed-up from evaluation at the subsystem level.

4.1. Mesh Refinement Study

The first step of the analysis is to perform a mesh refinement study to ensure that the governing equations of the mesh discretization are sufficiently converged. Mesh refinement is performed at both the subsystem level and coupled system level to demonstrate that the natural frequencies and SmEdA energies are sufficiently converged. The theoretical rate-of-convergence of a finite element mesh is observed when only one forward calculation is utilized; there is no guarantee for the coupled model to observe the same theoretical rate-of-convergence.

Table 2: Mesh Refinement of Higher-Order Tracked Frequency of the Four Subsystems

SS	$\Delta x = 2\,mm$		$\Delta x = 1\,mm$		$\Delta x = 0.5\,mm$		y_{Ref}	Convergence
	$y(\Delta x)$ (Hz.)	% Error	$y(\Delta x)$ (Hz.)	% Error	$y(\Delta x)$ (Hz.)	% Error		
1	2195.2	1.95	2224.7	0.63	2234.2	0.20	2238.8	1.63
2	2178.2	1.51	2197.0	0.66	2205.2	0.29	2211.5	1.20
3	2152.3	0.79	2165.1	0.20	2168.4	0.05	2169.5	1.97
4	2159.3	1.44	2180.7	0.46	2187.6	0.15	2190.9	1.64

The mesh refinement study is presented here based on the criteria at the subsystem level that natural frequencies of the subsystems around 2 kHz are estimated with less than 2% error, and at the coupled level that the number of modes and SmEdA energies have converged. The mesh criteria obtained at the subsystem level can be compared to classical approaches based on the wavelength but no similar method exists at the coupled level. The results of the mesh convergence of higher-order frequencies of the four subsystems are plotted in Figure 7, with the values obtained for the natural frequencies in Hz , the error in % shown in Table 2. The reference solution utilized in Table 2 is obtained using the Richardson extrapolation of the frequencies obtained using the three different mesh sizes, according to which the percent error is less than 2% for all mesh sizes investigated. Above the classical rule of thumb indicating that 6

elements by wavelength should be used, the analysis indicates that the mesh is fine enough to reach the converged zone. In this converged zone, a mesh size reduction is directly associated to a reduction of error in the quantity of interest. It is thus noted that 2% error of natural frequencies with values around 2 kHz will still result in a 40 Hz error. In comparison, the convergence of the SmEdA energies, and number of modes obtained in the frequency band 1410 - 1780 Hz is shown in Table 3 for all three mesh sizes investigated. For each mesh size, the obtained energy and the number of modes in the frequency band of interest are reported. It is chosen to use mesh size of $\Delta x = 1$ mm because the error in the natural frequencies is less than 1% and the number of modes in the frequency band appear to have converged.

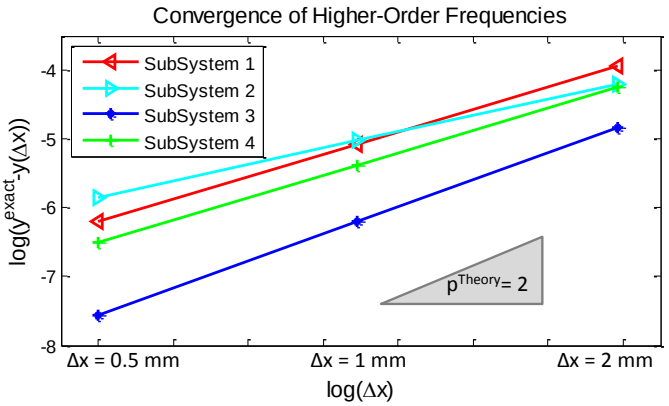

Figure 7: Mesh Refinement of Higher-Order Frequencies of the Four Subsystems.

Table 3: Mesh Refinement of SmEdA Energies of the Four Subsystems.

SS	$\Delta x = 2\,mm$		$\Delta x = 1\,mm$		$\Delta x = 0.5\,mm$	
	Energy (J)	Modes (no unit)	Energy (J)	Modes (no unit)	Energy (J)	Modes (no unit)
1	1.71e-6	61	1.72e-6	61	1.74e-6	62
2	3.41e-7	46	3.25e-7	43	3.09e-7	41
3	1.89e-6	24	1.89e-6	23	1.88e-6	23
4	9.38e-8	97	1.03e-7	94	1.05e-7	94

4.2. Effect Screening and Uncertainty Propagation at the Sub-System Level

The next part of the analysis proceeds with effect screening using the physical parameters at the sub-system level. The parameters pursued herein are listed previously in Table 1. For comparison, the three methods discussed in Section 3 are considered: (i) the finite differences approach, which provides a local measure of sensitivity, (ii) the correlation coefficients obtained from Monte Carlo sampling, and (iii) the Morris method. A visual comparison of the three approaches is provided in Figures 8 and 9.

The finite differences approach is pursued by perturbing each one of the sixteen parameters one at a time, by 1% of its relative value, requiring a total of 17 model simulations. In contrast, the correlation coefficients are obtained using 100 Monte Carlo simulations of the numerical model, whereby the sampling is defined using a latin-hypercube design of experiments, and each parameter is allowed to vary uniformly by ±15% from its nominal setting. A comparison of the parameter rankings in the frequency band of interest obtained using the finite differences approach and correlation coefficients is provided in Figure 8. Note that the color scale used in the two figures provides the relative influence of the parameter to the calculated SmEdA energies. The rankings obtained using the two approaches are clearly different. For the SmEdA energy of the first and second subsystems, the two approaches identify the thickness of the first and second plates, t_1 and t_2 to be most influential, and then the parameter ranking starts to deviate. For the SmEdA energy of the third subsystem, the finite difference approach identifies the Young's modulus and density of the third plate, E_3 and ρ_3 to be most influential whereas the thickness of the third and fourth plates, t_3 and t_4 are identified

by the correlation coefficients. For the fourth subsystem, the finite differences and correlation coefficients consistently identify the thickness of the third and fourth subsystems, t_3 and t_4, to be most influential.

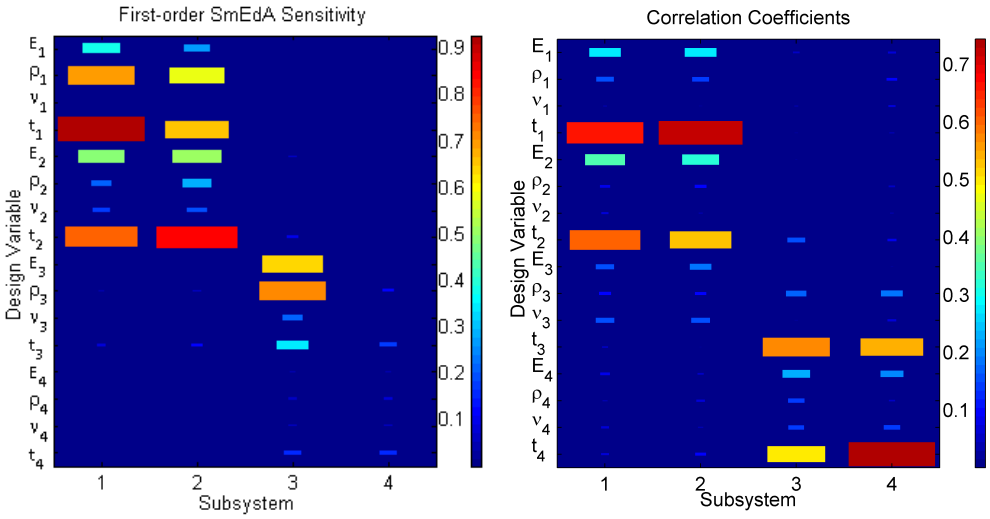

(a) Finite Differences (b) Correlation Coefficients

Figure 8: Comparison of Sensitivity Rankings.

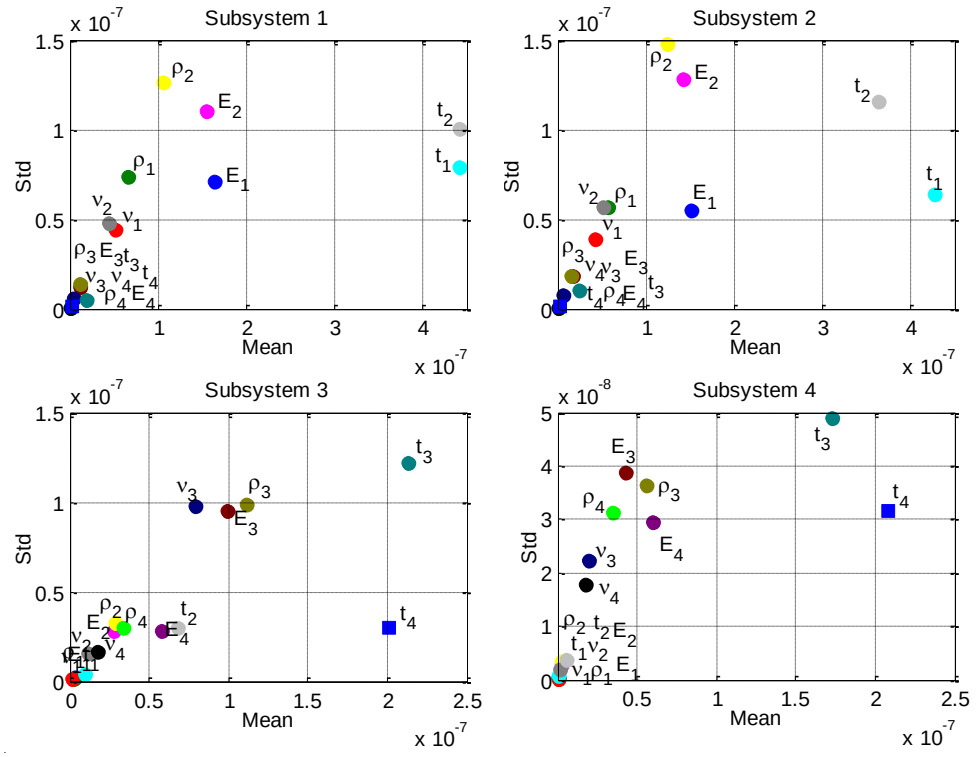

Figure 9: Morris Method Results.

The results obtained using thirty trajectories with the Morris method are provided in Figure 9. The simulation with thirty trajectories requires $30 \times (16 + 1) = 510$ simulations, in comparison with the 100 simulations utilized to determine the correlation coefficients. The graphics for conveying the results of the Morris method are considerably different than the results provided previously in Figure 8. This is due to the fact that the influence of each parameter is determined using the mean and standard deviation statistics of the elementary effects, thus requiring two axes to plot the results. It is noted that the most influential parameters obtained by the Morris method are consistent with those identified by the correlation coefficients.

A quantitative comparison of the parameters most influential to the SmEdA energy calculated for the third subsystem only is provided in Table 4. The mean and standard deviation statistics of the elementary effects obtained with the Morris method are both provided, however, the ranking obtained using the Morris method is ordered according the mean. Note that the ranking provided by each method is only qualitative. The two parameters identified as being most influential, t_3 and t_4 are consistent between the ranking provided by the correlation coefficients and the Morris method, however, the local measure of sensitivity utilized by the finite differences approach identifies ρ_3 and E_3 as being most influential instead. After the first two parameters, the ranking obtained for the correlation coefficients and Morris method becomes inconsistent. This can be explained by the fact that the standard deviation term, $\sigma_k(EE)$ is significant for the 3^{rd} to 5^{th} parameters identified as influential by the Morris method, suggesting that these parameters, ρ_3, E_3, and ν_3, are non-linear or that they are coupled to other influential effects. In contrast, the correlation coefficients are unable to account for higher-order interactions.

Table 4: Comparison of Ranking Results for the Third Subsystem

Ranking	Finite Differences		Correlation Coefficients		Morris Method		
	Parameter	$\frac{\partial y_i}{\partial \theta_j}$	Parameter	r_{xy}	Parameter	$\mu_k(EE)$	$\sigma_k(EE)$
1	ρ_3	0.7111	t_3	0.5784	t_3	2.14e-7	1.22e-7
2	E_3	-0.6439	t_4	-0.4967	t_4	2.01e-7	2.96e-8
3	t_3	-0.3375	E_4	-0.2379	ρ_3	1.11e-7	9.90e-8
4	ν_3	-0.2139	ρ_3	0.1746	E_3	9.96e-8	9.55e-8
5	t_4	-0.1642	t_2	-0.1524	ν_3	7.96e-8	9.76e-8
6	t_2	0.1036	ρ_4	-0.1415	t_2	6.76e-8	3.01e-7
7	ν_4	-0.0707	ν_4	-0.1341	E_4	5.83e-8	2.77e-8
8	E_2	0.0658	E_1	0.0555	ρ_4	3.38e-8	2.96e-8
9	ρ_4	0.0656	ν_1	0.0318	ρ_2	2.83e-8	3.28e-8
10	E_4	-0.0442	t_1	-0.0294	E_2	2.74e-8	2.80e-8
11	ρ_2	-0.0421	ν_3	0.0278	ν_4	1.75e-8	1.68e-8
12	ρ_1	0.0118	E_2	0.0173	ν_2	1.19e-8	1.55e-8
13	t_1	0.0056	E_3	0.0126	t_1	9.91e-9	4.04e-9
14	E_1	0.0054	ν_2	-0.0089	E_1	3.82e-9	2.38e-9
15	ν_1	-0.0029	ρ_1	-0.0051	ρ_1	2.17e-9	1.24e-9
16	ν_2	0.0023	ρ_2	0.0015	ν_1	1.15e-9	1.30e-9

4.3. Comparison of Uncertainty Propagation at the Subsystem and Coupled Model Levels

Uncertainty propagation at the coupled model level is pursued through application to the modal frequencies of the subsystem models. Doing so requires that the spatial bases of the modal frequencies are tracked to ensure that a parametric study at the coupled level will replicate the effect of modifying parameters at the subsystem level. For this reason, the frequency band is increased to 1100 - 2200 Hz to ensure that modal bases that might drift in or out of the frequency band of interest are tracked. The 100 Monte Carlo simulations used to approximate the correlation coefficients in Section 4.3 are used for generating the spatial modal bases of the expanded frequency band. Because the Monte Carlo simulations are re-used in this section, all of the parameters used to define the subsystems are varied to investigate the spatial modal bases for simulation at the coupled model level. A comparison of the number of mode shapes obtained for the original frequency band of the nominal model, and when the frequency band is expanded to track the modal bases are provided in Table 5. As shown in the table, the number of mode shapes increases from

221 for the original frequency band of the nominal model to 562 for the expanded frequency band used to track all potential modal bases.

Table 5: Number of Modal Bases for each Subsystem.

Sub-System	Nominal Frequency Band (1410 - 1780 Hz)	Monte Carlo Evaluations (1100 - 2200 Hz)
1	61	168
2	43	108
3	23	58
4	94	228
Total	221	562

According to the methodology for multi-variate sampling discussed previously in Section 3.4, a covariance matrix is used to inform the multivariate sampling of the natural frequencies. In this application, the covariance matrix has been obtained from the 100 Monte Carlo samples performed at the subsystem level and is mostly uniform. A preliminary investigation has been performed to check the convergence of the statistics of interest with 100 samples. The uniformity of the covariance matrix is likely due to the fact that the plates are assumed to be composed of linear, homogenous materials, and thus, variations of the physical parameters induce roughly similar variation in the natural frequencies. It is clearly appealing to utilize computation at the coupled model level due to the computational efficiency of bypassing the FE model evaluation; however, it is necessary first to verify whether evaluation at the coupled model level is capable of replicating results at the subsystem level. To exploit this computational efficiency, 5000 Monte Carlo samples at the coupled model level are performed and the calculated vibratory energies are compared to those obtained with the 100 Monte Carlo samples performed at the subsystem level.

Figure 10 provides a visual comparison of the vibratory energies obtained at the coupled model and subystem levels. The left image of Figure 10 shows the output-output plot of the energy obtained for the second and third subsystems, and the right image shows a comparison of histograms of energy calculated for the third subsystem. In the output-output scatter plot, the blue circles indicate samples obtained at the coupled model level, and the red circles indicate samples obtained at the subsystem model level. In the histogram, the red bars indicate sampling performed at the subsystem level, and the blue bars indicate sampling performed at the coupled model level. These plots clearly show that the Monte Carlo sampling at the coupled model level has a tendency to produce SmEdA energies that are outside of the distribution obtained at the subsystem level.

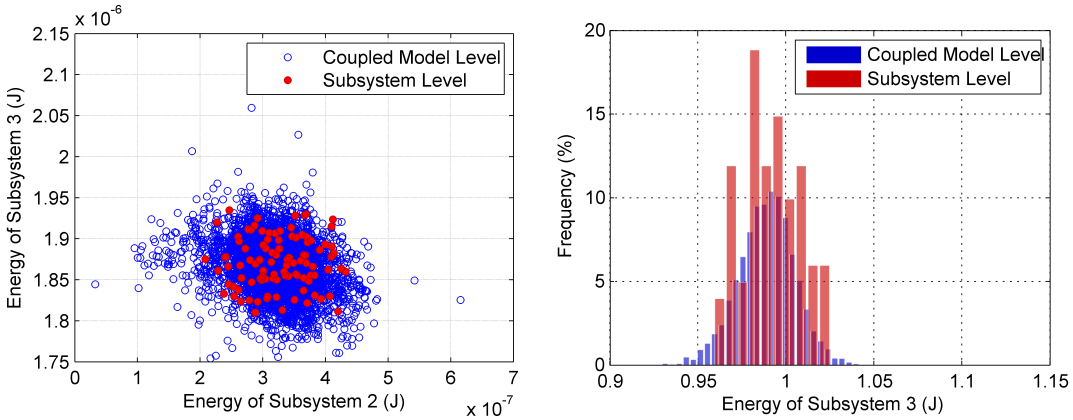

Figure 10: Output-Output Plot of Energy for the Second and Third Subsystems (left) and Third Subsystem Energy Histogram (right).

A figure showing the comparison of the energies obtained for all four subsystems is provided in Figure 11. The diagonal plots show the comparison of the histograms of SmEdA predictions for each subsystem,. The off-diagonal plots show the comparison of the output-output scatter plots obtained, where the row number defines which subsystem is plotted on the y-axis, and the column number defines which subsystem is plotted on the x-axis. The main conclusion

of Figure 11 is that the sampling provided at the coupled model level is able to capture the tendency of the predictions at the subsystem level, but with a larger overall spread of predictions.

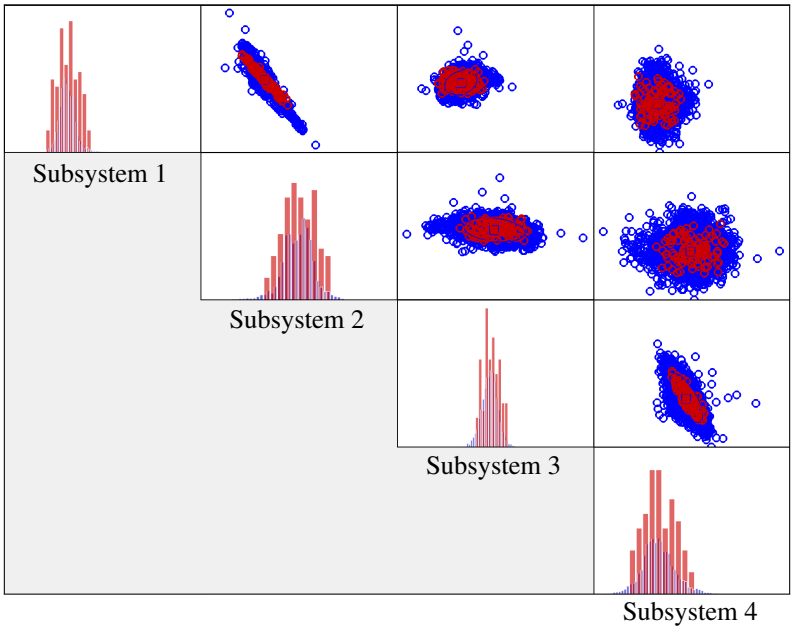

Figure 11: Comparison of Results Obtained from Monte Carlo Sampling at the Subsystem and Coupled Model Levels.

A quantitative comparison of the statistics obtained for the Monte Carlo sampling performed at the subsystem and coupled model levels are provided in Table 6. The consistency of the statistics demonstrate that the use of natural frequencies offers the potential to provide an adequate substitute to use of the input parameters for uncertainty propagation.

Table 6: Statistics of Monte Carlo Sampling.

Subsystem	Subsystem Model Calculated Energy (J)		Coupled Model Calculated Energy (J)	
	Mean	Standard Deviation	Mean	Standard Deviation
1	1.71e-6	5.66e-8	1.71e-6	4.21e-8
2	3.25e-7	5.24e-8	3.22e-7	5.03e-8
3	1.87e-6	3.08e-8	1.87e-6	3.11e-8
4	1.03e-7	2.45e-8	1.02e-7	2.57e-8

5. Conclusions of the proposed approach

The question at stake in this work is the level at which parametric studies can be applied when considering coupled problems involving two levels, the subsystem and the coupled model level. Choosing to pursue UQ at the subsystem level can be computationally expensive but the results are physically meaningful, whereas analysis performed at the coupled model level can be computationally trivial but with a less intuitive physical interpretation of the results. Furthermore, there is no guarantee that propagation of uncertainty at the coupled model level will be representative of the variability that would be obtained at the subsystem level. The proposed approach incorporates the use of a covariance matrix, informed by minimal sampling at the subsystem level, to propagate uncertainty at the coupled model level. Doing so makes it possible to maintain computational efficiency while simultaneously providing results that are physically meaningful to the analyst. The approach is applied on a four-subsystem model simulated in the Statistical Modal Energy Distribution Analysis (SmEdA) framework, an extension of the Statistical Energy Analysis

(SEA). The subsystem level inputs in this case are the material properties and geometry used to define the finite element models of the physical structure. There are two coupled model levels, the first being the natural frequencies and mode shapes obtained from the finite element model and the second being the coupling loss factors and internal loss factors calculated from the FE model results. A comparison of uncertainty propagation applied to the input parameters at the subsystem level and the natural frequencies at the coupled model demonstrates that the overall statistics of uncertainty propagation can be replicated using the coupled model level. However, due to the fact that the coupled model level can be sampled significantly times more than the subsystem level, the range of predictions is much larger. In the proposed work uncertainty has only been introduced in the natural frequencies. This is a reasonable assumption for the case-study application utilized herein, whereby the identity of the mode shapes likely stays consistent. Uncertainty of a mode shape for more complicated structures requires significantly more care than considering uncertainty of the scalar-valued natural frequencies. In addition, alternatives to the use of the covariance matrix to relate the output at the subsystem level to the inputs at the coupled model level can also be further explored. The fundamental assumption behind the covariance matrix is that the parameter space can be described using a multivariate random normal distribution. There is still an open-ended question as to whether this is the most appropriate formulation, and an area of future work would be to explore the effect of this assumption on the analysis result.

6. Concluding remarks

In this manuscript, uncertainty quantification (UQ) has been performed utilizing two different model form definitions that can be defined within a coupled model framework: (1) at the subsystem level whereby the model is parameterized using physical input parameters or (2) at the coupled model level using intermediate quantities of the analysis. To focus on the variability of model parameters and reduce the numerical uncertainty caused by truncation effects and mesh discretization in particular, preliminars studies on mesh refinement and effect screening are performed: covariance matrix-based uncertainty propagation at the subsystem level has proven to be time-efficient. The results of the UQ then show that quite similar results are obtained working at both the subsystem and the model coupled level, with a higher range of predictions at the coupled model level.

Acknowledgments

The authors acknowledge fundings from the FUI-CLIC project. It has been performed in cooperation with the Labex ACTION program (ANR-11-LABX-0001-01).

References

[1] R.H. Lyon and G. Maidanik. Power flow between linearly coupled oscillators. *The Journal of the Acoustical Society of America*, 34(5):623 – 639, 1962.

[2] R.H. Lyon and E. Eichler. Random vibration of connected structures. *The Journal of the Acoustical Society of America*, 36(7):1344 – 1354, 1964.

[3] R.H. Lyon and T.D. Scharton. Vibrational-energy transmission in a three-element structure. *The Journal of the Acoustical Society of America*, 38(2):253 – 261, 1965.

[4] F.J. Fahy. Statistical energy analysis: a critical overview. *Philosophical Transactions: Physical Sciences and Engineering*, 346(1681):431 – 447, 1994.

[5] T. Lafont, N. Totaro, and A. Le Bot. Review of statistical energy analysis hypotheses in vibroacoustics. *Proceedings of the Royal Society of London A: Mathematical, Physical and Engineering Sciences*, 470(2162):20130515, 2013.

[6] K. Renji. On the number of modes required for statistical energy analysis-based calculations. *Journal of Sound and Vibration*, 269(3-5):1128 – 1132, 2004.

[7] L. Maxit. *Extension et reformulation du mod èle SEA par la prise en compte de la répartition des énergies modales.French (tel-00777764)*. PhD thesis, L'Institut National des Sciences Appliques de Lyon, 2000.

[8] L. Maxit and J.L. Guyader. Extension of SEA model to subsystems with non-uniform modal energy distribution. *Journal of Sound and Vibration*, 265(2):337 – 358, 2003.

[9] S. De Rosa and F. Franco. On the use of the asymptotic scaled modal analysis for time-harmonic structural analysis and for the prediction of coupling loss factors for similar systems. *Mechanical Systems and Signal Processing*, 24(2):455 – 480, 2010.

[10] S. De Rosa, F. Franco, and T. Polito. Partial scaling of finite element models for the analysis of the coupling between short and long structural wavelengths. *Mechanical Systems and Signal Processing*, 5253:722 – 740, 2015.

[11] B. R. Mace and P. J. Shorter. Energy flow models from finite element analysis. *Journal of Sound and Vibration*, 233(3):369 – 389, 2000.

[12] D.A. Tortorelli and P. Michaeleris. Design sensitivity analysis: Overview and review. *Inverse Problems in Engineering*, 1(1):71 – 105, 1994.

[13] T.G Trucano, L.P. Swiler, T. Igusa, W.L. Oberkampf, and M. Pilch. Calibration, validation, and sensitivity analysis; what's what. *Reliability Engineering and System Safety*, 91(10-11):1331 – 1357, 2006.
[14] J.-L. Christen, M. N. Ichchou, B. Troclet, O. Bareille, and M. Ouisse. Global sensitivity analysis of analytical vibroacoustic transmission models. *Journal of Sound and Vibration*, 368:121 – 124, apr 2016.
[15] R.C. Smith. *Uncertainty Quantification: Theory, Implementation, and Applications*, volume 12. Society for Industrial and Applied Mathematics, 2013.
[16] A. Saltelli, K. Chan, and E.M. Scott. *Sensitivity analysis*, volume 134. Wiley New York, 2000.
[17] B. Moaveni, J.P Conte, and F.M. Hemez. Uncertainty and sensitivity analysis of damage identification results obtained using finite element model updating. *Computer-Aided Civil and Infrastructure Engineering*, 24(5):320 – 334, 2009.
[18] S. Atamturktur, F.M. Hemez, and J.A. Laman. Uncertainty quantification in model verification and validation as applied to large scale historic masonry monuments. *Engineering Structures*, 43:221–234, 2012.
[19] W. D'Ambrogio and A. Fregolent. Effect of uncertainties on substructure coupling: modelling and reduction strategies. *Mechanical Systems and Signal Processing*, 23(3):588 – 605, 2009.
[20] A. Saltelli and P. Annoni. How to avoid a perfunctory sensitivity analysis. *Environmental Modelling and Software*, 25(12):1508 – 1517, 2010.
[21] A.N. Thite and B.R. Mace. Robust estimation of coupling loss factors from finite element analysis. *Journal of Sound and Vibration*, 303(3-5):814 – 831, 2007.
[22] A. Sarkar and R. Ghanem. Mid-frequency structural dynamics with parameter uncertainty. *Computer Methods in Applied Mechanics and Engineering*, 191(4748):5499 – 5513, 2002.
[23] B. Van den Nieuwenhof and J-P. Coyette. Modal approaches for the stochastic finite element analysis of structures with material and geometric uncertainties. *Computer Methods in Applied Mechanics and Engineering*, 192(3334):3705 – 3729, 2003.
[24] C.J. Radcliffe and X.L. Huang. Putting statistics into the statistical energy analysis of automotive vehicles. *Journal of Vibration and Acoustics*, 119(4):629 – 634, 1997.
[25] C. Soize. Random uncertainties modeling for the medium-frequency dynamics. In WQ Zhu, GQ Cai, and RC Zhang, editors, *5th International Conference on Stochastic Structural Dynamics*, pages Pages: 429–436, Hangzou, China, August 2003. Zhejiang University, CRC Press-Taylor & Francis Group, 6000 Broken Sound Parkway NW, STE 300, Boca Raton, FL 33487-2742 USA.
[26] A. Culla, W. D'Ambrogio, and A. Fregolent. Parametric approaches for uncertainty propagation in SEA. *Mechanical Systems and Signal Processing*, 25(1):193 – 204, 2011.
[27] M. Xu, Z. Qiu, and X. Wang. Uncertainty propagation in sea for structural-acoustic coupled systems with non-deterministic parameters. *Journal of Sound and Vibration*, 333(17):3949 – 3965, 2014.
[28] Z. Qiu and X. Wang. Comparison of dynamic response of structures with uncertain-but-bounded parameters using non-probabilistic interval analysis method and probabilistic approach. *International Journal of Solids and Structures*, 40(20):5423 – 5439, 2003.
[29] FM Hemez and JR Kamm. A brief overview of the state-of-the-practice and current challenges of solution verification. In *Computational Methods in Transport: Verification and Validation*, pages 229–250. Springer, 2008.
[30] M.D. Morris. Factorial sampling plans for preliminary computational experiments. *Technometrics*, 33(2):161 – 174, 1991.
[31] F. Camolongo, J. Cariboni, and A. Saltelli. An effective screening design for sensitivity analysis of large models. *Environmental Modelling and Software*, 22(10):1509 – 1518, 2007.